



Cite this: *Chem. Sci.*, 2025, **16**, 19187

All publication charges for this article have been paid for by the Royal Society of Chemistry

Received 20th April 2025
Accepted 26th August 2025

DOI: 10.1039/d5sc02879e
rsc.li/chemical-science

Identification of a photoredox-active Pt(IV) complex that induces light-mediated cell death

Jevon W. Marsh,[†]^a Lina Hacker,[†]^b Sophie A. Twigger,[†]^b Jake A. Vickery,[†]^b Shitong Huang,^a Claudia Almuzara Romero,^c Aaron P. Langston,^c Ismael Diez-Perez,[†]^b Rebecca A. Musgrave,[†]^b Ester M. Hammond,[†]^b and Adam C. Sedgwick[†]^{b*}^{ac}

We report the synthesis and characterisation of a series of fluorogenic Pt(IV) complexes – **CarboBlue**, **OxaliBlue** and **CisBlue**. These Pt(IV) complexes were identified as photoactive, oxidising biomolecules under light irradiation to then undergo rapid intramolecular photoreduction to release the fluorescent reporter, Nap-OH and corresponding Pt(II) species. **OxaliBlue** and **CisBlue** displayed cytotoxicity regardless of light irradiation. In contrast, HCT116 cells treated with **CarboBlue** displayed a light-dependent increase in fluorescence emission along with selective light-induced toxicity.

Pt(IV) complexes hold promise as potential cancer-selective alternatives to the FDA-approved Pt(II) chemotherapeutics, cisplatin, oxaliplatin, and carboplatin.^{1,2} It is widely considered that Pt(IV) complexes are non-toxic prodrugs that undergo intracellular reduction to afford the corresponding cytotoxic Pt(II) species. However, the exact mechanism for Pt(IV) reduction within cells remains poorly understood. Given that the mode of activation directly determines the selectivity and efficacy of these compounds, a comprehensive understanding of Pt(IV) redox chemistry within biology is needed. To address this knowledge gap, significant research efforts have been made towards identifying factors that contribute to Pt(IV) activation within cells.^{3–6} Notably, fluorogenic Pt(IV)-based probes have been developed by incorporating fluorophores at the axial positions.^{7–9} Reductive activation of these fluorogenic Pt(IV) complexes enables direct visualisation of intracellular Pt(IV) reduction *via* the release of the fluorescent axial ligand(s), affording an “off” to “on” fluorescence response.^{7,10} To this end, our group recently visualised the hypoxia-mediated reduction of fluorogenic Pt(IV) complexes (e.g., **CarboNap** (Fig. 1)),^{11,12} which in turn has informed the design of so-called Hypoxia-Activated Pt(IV) Prodrugs.¹¹ Hypoxia (low-oxygen concentrations) is a hallmark trait of many solid tumours,¹³ therefore this prodrug approach provides the potential to afford cancer-selective agents and overcome the systemic toxicity associated with traditional Pt(II) therapies.¹⁴ However, Pt(IV) prodrugs typically

display slow reduction kinetics, which impacts the overall translational potential of this strategy.¹⁵ To increase our understanding on intracellular Pt(IV) activation rates, in this work, we developed a series of fluorogenic Pt(IV) complexes, named **CarboBlue**, **OxaliBlue** and **CisBlue**. Given that light irradiation is an established method for accelerating Pt(IV) activation,^{4,16–19} we investigated and compared both light exposure and intracellular oxygen levels as activation mechanisms. Among these complexes, **CarboBlue** emerged as a promising photoactivated chemotherapeutic, demonstrating light as the dominant activation pathway.

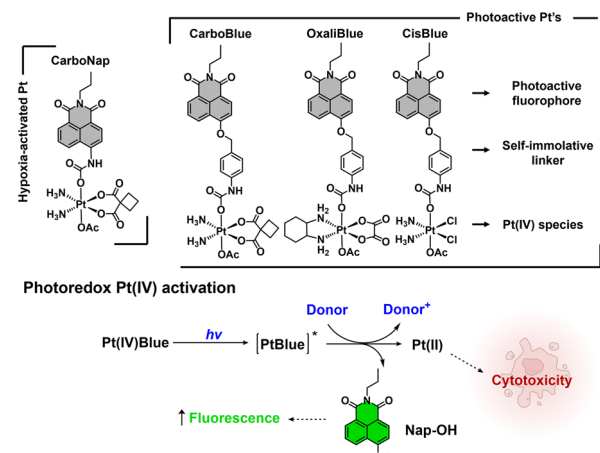


Fig. 1 Top: chemical structures of hypoxia-activated **CarboNap**, and light-activated **CarboBlue**, **OxaliBlue** and **CisBlue**. Below: general schematic of the proposed mechanism of the photoreduction of Pt(IV) complexes, releasing fluorescent reporter Nap-OH and cytotoxic Pt(II) species.

^aChemistry Research Laboratory, University of Oxford, Mansfield Road, Oxford, OX1 3TA, UK

^bDepartment of Oncology, University of Oxford, Old Road Campus Research Building, Oxford, OX3 7DQ, UK

^cDepartment of Chemistry, King's College London, 7 Trinity Street, London, SE1 1DB, UK. E-mail: adam.sedgwick@kcl.ac.uk

† These authors contributed equally.

In this study, the green-emitting fluorophore 4-hydroxy-*N*-propyl-1,8-naphthalimide (**Nap-OH**) was chosen. Several reports have demonstrated functionalisation of **Nap-OH** with stimuli-responsive self-immolative (traceless) linkers²⁰ to afford ratiometric fluorescent probes with a measurable change from blue to green emission.^{21,22} This ratiometric feature is desirable as it would enable the potential monitoring of both Pt(IV) species (blue emission) and the release of Pt(II) species (green emission). In brief, **Nap-OH** was synthesised following an established synthetic protocol by Pfeffer and co-workers,²³ and the desired fluorogenic Pt(IV) complexes, **CarboBlue**, **OxaliBlue** and **CisBlue** were isolated following established synthetic protocols (Schemes S1–S3).^{24,25} The full synthetic procedures and characterisation can be found in the SI.

While synthetic intermediate **Nap-Bn-COOH** (Scheme S1), displayed the expected blue emission, the Pt(IV)-functionality on **CarboBlue**, **OxaliBlue** and **CisBlue** resulted in significant fluorescent quenching of the blue fluorescence emission intensity (Fig. S1 and Scheme S4). This observed fluorescence quenching by Pt(IV) is attributed to the heavy-atom effect and the detection of singlet oxygen production from **CarboBlue** is suggestive of potential intersystem crossing of the singlet excited state (Fig. S2).^{10,26} Due to the quenching of the blue emissive states, we therefore focused on monitoring the changes in fluorescence emission at the expected 550 nm emission of **Nap-OH** with and without sodium ascorbate (NaAsc).²² **CarboBlue**, **OxaliBlue**, and **CisBlue** were separately incubated with NaAsc (10 mM, 1 h) in PBS buffer (pH = 7.4, 0.01 M) and the fluorescence emission intensity at 550 nm was monitored every 10 minutes over a time period of 1 hour. Surprisingly, when compared to our previously reported hypoxia-activated **CarboNap**,¹¹ which readily activates with NaAsc, only **CisBlue** showed a noticeable increase in fluorescence emission intensity (12.3 fold-change); minimal fluorescence changes were observed for **OxaliBlue** and **CarboBlue** (Fig. 2a and S3–S5). Considering these newly synthesised complexes lacked sensitivity towards NaAsc-mediated reduction, we wanted to understand the differences in reactivity compared to NaAsc-sensitive **CarboNap**.¹¹ Cyclic voltammetry experiments were performed and the reduction potentials (cathodic peaks) of **CarboBlue** and **OxaliBlue** were measured in DMF as -0.35 , and -0.21 vs. Fc^0/Fc^+ , respectively (Fig. S6). Efforts to obtain a suitable reduction potential for **CisBlue** proved difficult due to solubility issues. However, in the instance of **CarboNap** under the same measurement conditions, a more positive reduction potential (-0.005 V vs. Fc^0/Fc^+) was observed supporting its observed greater sensitivity towards NaAsc-mediated reduction (Fig. S7).

Next, the reactivity of **CarboBlue**, **OxaliBlue** and **CisBlue** towards light-mediated reduction was tested. An aqueous solution (PBS, pH = 7.4, 0.01 M) of each complex (5 μ M) was subjected to blue light irradiation (spectral width: 400–500 nm, 4 W, 1 h) and fluorescent measurements were studied over the same time course. As seen in Fig. 2b and S8–S10, increasing the length of light exposure time resulted in gradual increases in fluorescence emission intensities at 550 nm. In contrast, the co-treatment of light irradiation and NaAsc (10 mM) resulted in

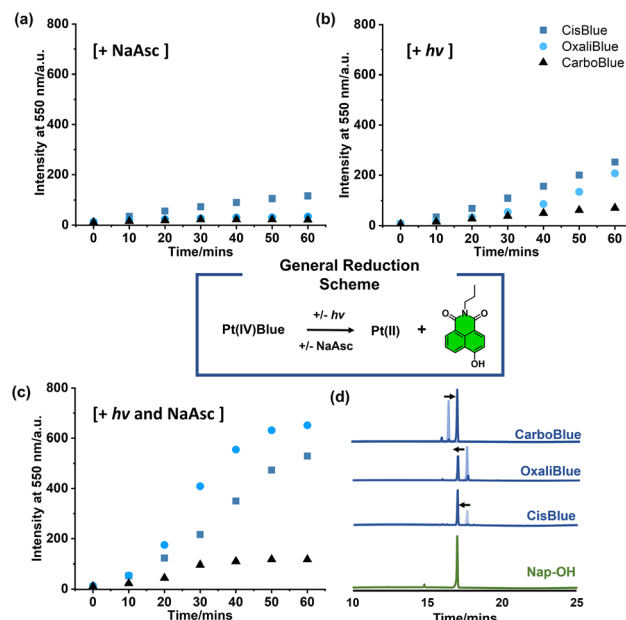


Fig. 2 Changes in fluorescence emission intensity of **CisBlue**, **OxaliBlue** and **CarboBlue** (all 5 μ M) at 550 nm over time (0, 10, 20, 30, 40, 50, and 60 min) (a) incubated with NaAsc (10 mM), (b) irradiated with blue light and (c) irradiated with blue light in the presence of NaAsc (10 mM). (d) HPLC chromatograms of **Nap-OH** (green), **CisBlue**, **OxaliBlue** and **CarboBlue** (all blue) (all 50 μ M) irradiated with blue light and incubated with NaAsc (50 mM) for 1, 2 and 4 h, respectively, superimposed with their initial 0 h timepoint (shaded blue). All fluorescence spectra were performed in PBS (pH = 7.4, 0.01 M), $\lambda_{\text{ex}} = 450$ nm, slit widths: 10 nm and 5 nm; HPLC studies were performed in a $\text{H}_2\text{O}/\text{MeCN}$ (70/30%) solution.

much greater changes in fluorescence emission when compared to light irradiation or NaAsc alone (Fig. 2c and S11–S13), with a 54.2, 52.0 and 7.96-fold-change for **CisBlue**, **OxaliBlue** and **CarboBlue**, respectively. A trend in reactivity was observed; **CarboBlue** was found least reactive and required higher concentrations of NaAsc (50 mM) with light irradiation to observe noticeable increases in fluorescence emission (Fig. S11). This synergistic effect between light and NaAsc was further validated via UV-Vis spectroscopy (Fig. S14–S16) and HPLC analysis (Fig. 2d and S17–S19). Minimal change to the fluorescence emission spectra and HPLC traces were seen in the absence of light and reductant, suggestive of good aqueous stability (Fig. S20–S25).

With the above data showcasing the potential of these complexes as promising photoactivated chemotherapeutics, we wanted to first determine the dark cytotoxicity of each complex (without light irradiation). In the absence of light, both **CisBlue** and **OxaliBlue** (10 μ M) demonstrated significant cytotoxicity in a colorectal cancer cell line (HCT116). However, at the same concentration, **CarboBlue** appeared non-toxic after an incubation period of 64 h (Fig. S26). For these reasons, only **CarboBlue** was investigated further in this study.

In an effort to understand the photochemistry of **CarboBlue**, the excited-state reduction potential was estimated by combining the electrochemical and spectroscopic data



(Fig. S27),^{19,27} which was calculated as 2.77 V vs. Fc^0/Fc^+ . Interestingly, the excited-state reduction potential of previously reported **CarboNap** was calculated to be 2.86 V, which led to the identification of a similar light-mediated activation mechanism (Fig. S28 and S29). Time-dependent density functional theory (TD-DFT) calculations and natural transition orbitals (NTOs) identified excited states (>400 nm) for both **CarboNap** and **CarboBlue** corresponding to a ligand-to-metal charge transfer (LMCT)²⁸ involving a ligand-based π orbital and the Pt $\text{d}z^2$ -based orbital, which supports the observed photomediated reduction mechanism for **CarboNap** and **CarboBlue** (See SI – computational analysis). Notably, the calculated excited-state properties of **CarboBlue** also suggested potential photooxidative behaviour, reinforcing the role of NaAsc as a sacrificial electron donor to facilitate and accelerate intramolecular photoreduction.^{19,29} **CarboBlue** was therefore next tested with the known biological electron donor, NADH. The light irradiation of **CarboBlue** with increasing concentrations of NADH (0–4 mM) resulted in a dose-dependent increase in fluorescence emission intensity at 550 nm (blue lines: light + NADH, black line: light only, Fig. 3). High-resolution mass spectrometry and fluorescence spectroscopy (NADH emission) supported the potential photooxidation of NADH to NAD^+ via **CarboBlue** (Fig. S30–S32). Other biologically reducing species such as L-cysteine were also found to enhance the light-mediated increases in fluorescence emission intensities for **CarboBlue** (Fig. S33). Thus, with the known abundance of biological reductants in cancer cells,³⁰ we believe these findings warranted testing **CarboBlue** as a potential phototherapeutic in cell studies.

Fluorescence imaging is crucial to understanding the influence of light and oxygen concentrations on the activation of **CarboBlue** within cells. As anticipated, HCT116 cells treated with **CarboBlue** and NaAsc (2 mM), followed by light irradiation (400–500 nm, 4 W, 30 min), resulted in significant enhancement

in fluorescence emission intensity (determined by flow cytometry) (Fig. S34). We next wanted to determine and compare the ability of **CarboBlue** to undergo hypoxia-mediated reduction against light-mediated activation. HCT116 cells were treated with **CarboBlue** (2.5, 5, 10 μM) for 16 h at 21%, or $<0.1\%$ O_2 and then analysed *via* flow cytometry (Fig. 4a). Unlike our previously reported fluorogenic Pt(IV) complexes,^{11,12} no significant difference was observed in fluorescence emission intensity between 21% and $<0.1\%$ O_2 concentrations, suggestive of no hypoxia-mediated activation. However, when HCT116 cells were treated with **CarboBlue** (10 μM) and irradiated with light under

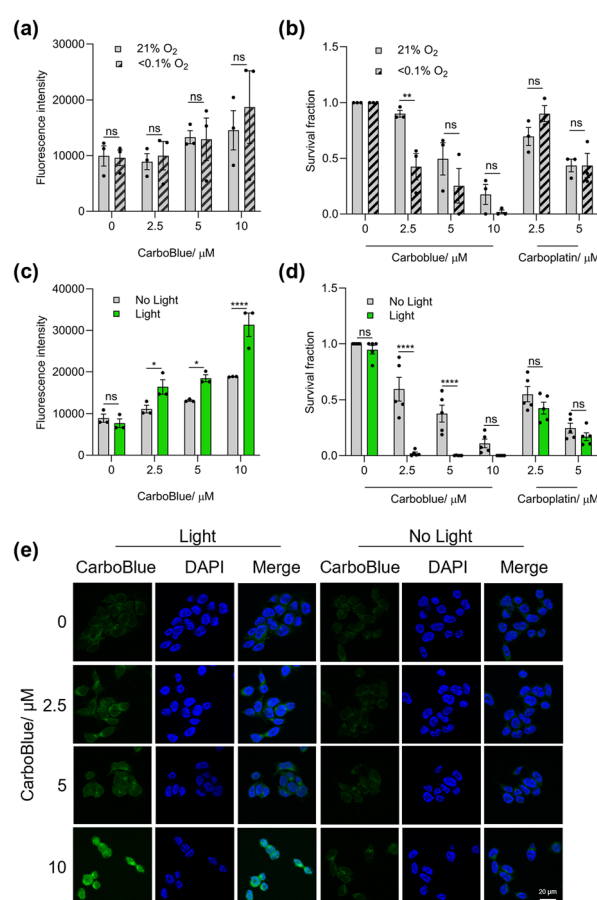


Fig. 4 HCT116 cells treated with **CarboBlue** (0, 2.5, 5, 10 μM) for 16 h (a) under 21 or $<0.1\%$ O_2 and analysed *via* flow cytometry (b) colony survival assay under 21 or $<0.1\%$ O_2 and then incubated at 21% O_2 (media changed after an additional 48 h) including carboplatin (2.5, 5 μM) (c) under 21% O_2 and then exposed to blue light (>400 nm) (30 min) before analysis *via* flow cytometry – light is shown by green bar (d) under 21% O_2 and then exposed to blue light (>400 nm) (30 min), media was then changed after an additional 48 h and a colony survival assay was undertaken (e) under 21% O_2 and then exposed to blue light (400 nm) (30 min) before analysis *via* confocal microscopy, with representative pictures shown (scale bar = 20 μm). Data shown in a, b, c and d are $n \geq 3$ and e is $n = 1$. Black dots on the graphs shown represent biological repeats (each of which was carried out in triplicate), and data is presented as mean \pm SEM. Statistical testing was done using two-way ANOVAs, where ns = non-significant, $*p < 0.05$, $**p < 0.01$, $****p < 0.0001$.

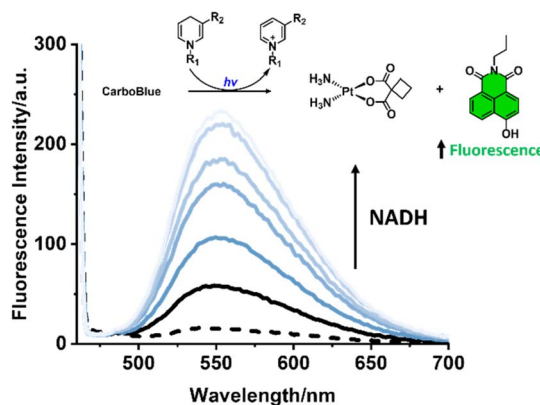


Fig. 3 General reduction scheme of **CarboBlue** irradiated with blue light and NADH to release Pt(II), Nap-OH and NAD^+ . Fluorescence emission spectra of **CarboBlue** alone (dashed line); (ii) **CarboBlue** irradiated with blue light (black); and (iii) **CarboBlue** irradiated with blue light with increasing concentrations of NADH (0.05, 0.1, 1, 2, and 4 mM, blue) for 1 h in PBS (pH = 7.4, 0.01 M), $\lambda_{\text{ex}} = 450$ nm, slit widths: 10 nm and 5 nm.

normoxic (21% O₂) and hypoxic conditions (<0.1% O₂), increases in fluorescent emission were observed regardless of oxygen concentrations (Fig. S35), indicating light as the most effective method for the activation of **CarboBlue** in cells.

While fluorescence analysis offers insight into the rate of Pt(IV) activation and a preliminary indication of the phototherapeutic potential of **CarboBlue**, accurate assessment of the efficacy of Pt-based therapeutics requires significantly longer evaluation periods (>24 hours).³¹ We therefore needed to determine whether the fluorescence response of **CarboBlue** exposed to light or hypoxic conditions correlated to cytotoxicity. Even though previously we had shown **CarboBlue** having minimal impact on cell viability, MTT assays do not accurately reflect long-term cell survival, as it primarily measures metabolic activity. Clonogenic assays are considered the gold standard for assessing long-term cell survival and provide a more comprehensive assessment of the long-term effects of Pt-based drugs.³² For these reasons, we evaluated the cytotoxicity of **CarboBlue** *via* a colony survival assay. HCT116 cells were treated with **CarboBlue** at various concentrations (2.5, 5, 10 µM) and conditions (hypoxia or blue light), and after 48 h, the plates were incubated at 21% O₂ to allow colonies to form (14 days). While no hypoxia-mediated increase in fluorescence emission was observed, **CarboBlue** displayed modest hypoxia-induced cytotoxicity (Fig. 4b). In addition, with increasing concentrations of **CarboBlue**, an increase in dark toxicity was observed. Since imaging experiments are conducted over a much shorter time-scale than colony survival assays (16 hours *vs.* 14 days), the observed increase in cytotoxicity suggests that intracellular reduction may occur progressively over the full duration of the 14 day study. Nonetheless, **CarboBlue** (2.5, 5, 10 µM) with light irradiation displayed significantly greater cytotoxicity (Fig. 4d). Confocal microscopy further confirmed the increase in fluorescence emission intensity of **CarboBlue** upon light irradiation (Fig. 4e) showcasing excellent intracellular photoactivation. Together with the synthetic versatility of the **Nap-OH** fluorescent scaffold, these findings support the potential of **CarboBlue** as a promising platform for optimisation as a photoactivated chemotherapeutic.³³

In conclusion, we report the synthesis of novel light-activated Pt(IV) complexes—**CarboBlue**, **OxaliBlue**, and **Cis-Blue**. Functionalisation of the **Nap-OH** fluorophore with Pt(IV) resulted in pronounced quenching of blue fluorescence emission, suggestive of potential intersystem crossing (*via* singlet oxygen detection) and the initiation of an intramolecular photoredox process. TD-DFT calculations and analysis of natural transition orbitals (NTOs) identified a ligand-to-metal charge transfer (LMCT) band around ~400 nm for **CarboBlue**. Comparable calculations also revealed an additional photo-mediated reduction pathway in our previously reported **Carbo-Nap**. Upon light irradiation, **CarboBlue**-treated HCT116 cells exhibited fluorescence turn-on, consistent with intracellular activation. In parallel, **CarboBlue** demonstrated significant cytotoxicity under light irradiation, underscoring its potential as a photoactivated chemotherapeutic. Collectively, this study highlights the non-innocent nature of chromophores and proposes a broader design strategy for photoactivated Pt(IV)

therapeutics through the simple conjugation of Pt(IV) complexes with known fluorophores.

Author contributions

JWM synthesised all the compounds and carried out the solution experiments shown in the study. LH and SAT conducted all cellular experiments. JAV, SH and APL performed background experiments to support the direction of the project. CAR, IDP and RAM provided support for electrochemical and theoretical experiments. JWM, EMH and ACS designed the experiments and analysed the data. Both JWM and ACS contributed to writing the manuscript.

Conflicts of interest

There are no conflicts to declare.

Data availability

Data will be made available by the corresponding authors upon request.

Supplementary information is available: Detailed procedures, characterisation, and NMR spectra are provided in the ESI. See DOI: <https://doi.org/10.1039/d5sc02879e>.

References

- 1 T. C. Johnstone, K. Suntharalingam and S. J. Lippard, *Chem. Rev.*, 2016, **116**, 3436–3486.
- 2 G. Thiabaud, G. He, S. Sen, K. A. Shelton, W. B. Baze, L. Segura, J. Alaniz, R. Munoz Macias, G. Lyness, A. B. Watts, H. M. Kim, H. Lee, M. Y. Cho, K. S. Hong, R. Finch, Z. H. Siddik, J. F. Arambula and J. L. Sessler, *Proc. Natl. Acad. Sci. U. S. A.*, 2020, **117**, 7021–7029.
- 3 S. Chen, Q. Zhou, K.-Y. Ng, Z. Xu, W. Xu and G. Zhu, *Inorg. Chem. Front.*, 2024, **11**, 3085–3118.
- 4 C. Imberti, J. Lok, J. P. C. Coverdale, O. W. L. Carter, M. E. Fry, M. L. Postings, J. Kim, G. Firth, P. J. Blower and P. J. Sadler, *Inorg. Chem.*, 2023, **62**, 20745–20753.
- 5 A. Lasorsa, O. Stuchlíková, V. Brabec, G. Natile and F. Arnesano, *Mol. Pharm.*, 2016, **13**, 3216–3223.
- 6 A. M. D. S. Jayawardhana and Y.-R. Zheng, *Dalton Trans.*, 2022, **51**, 2012–2018.
- 7 Y. Song, K. Suntharalingam, J. S. Yeung, M. Royzen and S. J. Lippard, *Bioconjug. Chem.*, 2013, **24**, 1733–1740.
- 8 H. Yao, S. Chen, Z. Deng, M.-K. Tse, Y. Matsuda and G. Zhu, *Inorg. Chem.*, 2020, **59**, 11823–11833.
- 9 H. Yao and G. Zhu, *Dalton Trans.*, 2022, **51**, 5394–5398.
- 10 J. J. Wilson and S. J. Lippard, *Inorg. Chim. Acta*, 2012, **389**, 77–84.
- 11 J. W. Marsh, L. Hacker, S. Huang, M. H. C. Boulet, J. R. G. White, L. A. W. Martin, M. A. Yeomans, H.-H. Han, I. Diez-Perez, R. A. Musgrave, E. M. Hammond and A. C. Sedgwick, *Dalton Trans.*, 2024, **53**, 14811–14816.
- 12 M. H. C. Boulet, H. R. Bolland, E. M. Hammond and A. C. Sedgwick, *J. Am. Chem. Soc.*, 2023, **145**, 12998–13002.



13 Z. Chen, F. Han, Y. Du, H. Shi and W. Zhou, *Signal Transduct. Targeted Ther.*, 2023, **8**, 70.

14 F. W. Hunter, B. G. Wouters and W. R. Wilson, *Br. J. Cancer*, 2016, **114**, 1071–1077.

15 S. Chen, H. Yao, Q. Zhou, M.-K. Tse, Y. F. Gunawan and G. Zhu, *Inorg. Chem.*, 2020, **59**, 11676–11687.

16 Z. Deng, N. Wang, Y. Liu, Z. Xu, Z. Wang, T.-C. Lau and G. Zhu, *J. Am. Chem. Soc.*, 2020, **142**, 7803–7812.

17 D. Spector, K. Pavlov, E. Beloglazkina and O. Krasnovskaya, *Int. J. Mol. Sci.*, 2022, **23**, 14511.

18 S. Huang, J. W. Marsh, J. R. G. White, T. Q. Ha, S. A. Twigger, I. Diez-Perez and A. C. Sedgwick, *New J. Chem.*, 2024, **48**, 7548–7551.

19 Z. Deng, H. Li, S. Chen, N. Wang, G. Liu, D. Liu, W. Ou, F. Xu, X. Wang, D. Lei, P. C. Lo, Y. Y. Li, J. Lu, M. Yang, M. L. He and G. Zhu, *Nat. Chem.*, 2023, **15**, 930–939.

20 J. Yan, S. Lee, A. Zhang and J. Yoon, *Chem. Soc. Rev.*, 2018, **47**, 6900–6916.

21 H. Zhu, C. Liu, M. Su, X. Rong, Y. Zhang, X. Wang, K. Wang, X. Li, Y. Yu, X. Zhang and B. Zhu, *Coord. Chem. Rev.*, 2021, **448**, 214153.

22 C. Liu, C. Shao, H. Wu, B. Guo, B. Zhu and X. Zhang, *RSC Adv.*, 2014, **4**, 16055–16061.

23 E. E. Rudebeck, R. P. Cox, T. D. M. Bell, R. Acharya, Z. Feng, N. Gueven, T. D. Ashton and F. M. Pfeffer, *Chem. Commun.*, 2020, **56**, 6866–6869.

24 V. E. Y. Lee, Z. C. Lim, S. L. Chew and W. H. Ang, *Inorg. Chem.*, 2021, **60**, 1823–1831.

25 G. A. Farrow, M. Quick, S. A. Kovalenko, G. Wu, A. Sadler, D. Chekulaev, A. A. P. Chauvet, J. A. Weinstein and N. P. Ernsting, *Phys. Chem. Chem. Phys.*, 2021, **23**, 21652–21663.

26 W.-P. To, Y. Liu, T.-C. Lau and C.-M. Che, *Chem.-Eur. J.*, 2013, **19**, 5654–5664.

27 W. E. Jones Jr and M. A. Fox, *J. Phys. Chem.*, 1994, **98**, 5095–5099.

28 A. M. May and J. L. Dempsey, *Chem. Sci.*, 2024, **15**, 6661–6678.

29 S. Abuhadba, C. Fuqua, A. Maltese, C. Schwinn, N. Lin, A. Chen, R. Martzloff, T. V. Esipova and T. Mani, *J. Am. Chem. Soc. Au*, 2024, **4**, 4892–4898.

30 R. Zhang, R. Kang and D. Tang, *Cancer Gene Ther.*, 2023, **30**, 929–931.

31 M. N. Brodeur, K. Simeone, K. Leclerc-Deslauniers, H. Fleury, E. Carmona, D. M. Provencher and A.-M. Masson, *Sci. Rep.*, 2021, **11**, 18183.

32 B. N. Forgie, R. Prakash, A. A. Goyeneche and C. M. Telleria, *Discov. Oncol.*, 2024, **15**, 5.

33 S. Bonnet, *Dalton Trans.*, 2018, **47**, 10330–10343.

